REVISITING JOINT STATISTICAL PROPERTIES OF SURF PARAMETER WITH CHARACTERISTIC WAVE PARAMETERS FOR SINGLE RANDOM WAVES INCLUDING SPECTRAL BANDWIDTH EFFECTS

Dag Myrhaug[1*], Hong Wang[1], Lars Erik Holmedal[1], Hongtao Li[2]

[1] Department of Marine Technology

[2] Department of Civil and Environmental Engineering

Norwegian University of Science and Technology (NTNU), Trondheim, Norway.

*Corresponding author at:
Department of Marine Technology, Norwegian University of Science and Technology (NTNU), Otto Nielsens vei 10, NO-7491, Trondheim.
E-mail address: dag.myrhaug@ntnu.no

Abstract

Results from a comparative study of the joint distribution of surf parameter and wave period are provided. The transformed Myrhaug and Kjeldsen (1984) joint distribution of wave height and wave period is compared with the transformed Longuet-Higgins (1983) joint distribution of wave height and wave period. The Myrhaug and Kjeldsen (1984) distribution is a parametric model originating from a best fit to relatively broad-band field data, whilst the Longuet-Higgins (1983) distribution is theoretically based. It appears that the theoretically based distribution does not represent the features of the parametric model especially well, suggesting that parametric models should be used to describe relatively broad-banded data.

Then, in order to study the effects of the spectral bandwidth the Longuet-Higgins (1983) joint distribution of wave height and wave period is transformed to obtain the joint distribution of surf parameter with wave height and wave period, as well as the joint distribution of wave runup time and wave period. Finally, comparisons are made with results from small-scale laboratory experiments related to stability of rubble-mound breakwaters provided by Sawaragi et al. (1982). The comparison between measurements and predictions of the distribution of the surf parameter is favorable, whilst the agreement is poorer for the probability of resonance.

Keywords: Surf parameter; Wave height; Wave period; Wave runup time; Joint distribution; Rubble-mound breakwaters.

1. Introduction

Waves that approach a coastline usually break and run up the coast, whether it is a structure or a beach. For land areas which are particularly exposed and vulnerable to waves this can cause flooding, serious coastal erosion/accretion impacting the shoreline configuration, as well as damage to coastal infrastructure such as seawalls, breakwaters, sand barriers and artificial reefs. The recent years focus on climate change and the possible consequences of more extreme weather and sea level rise has led to increased attention of these issues, see e.g. de la Pena et al. (2014), Blenkinsopp et al. (2016), Poate et al. (2016), Atkinson et al. (2017).

The surf parameter, also referred to as the Iribarren number, is often used to characterize physical processes in the surf zone. It is defined as the ratio between the slope of a beach (or a coastal structure) and the square root of the deep water wave steepness, and was introduced originally by Iribarren and Nogales (1949) and applied later by Battjes (1974). The surf zone is located in shallow water regions where waves break, and types of breakers on slopes are often

classified by the surf parameter (Battjes, 1974). The dissipation associated with wave breaking, turbulence and bottom friction leads to loss of energy causing the wave height to decrease towards the shoreline within the surf zone. Nearshore circulation is also affected by wave breaking as it contributes to strong currents along shorelines. The high turbulence level due to breaking waves also leads to intense sediment transport in the surf zone. Wave runup and wave rundown on beaches and coastal structures such as breakwaters, seawalls, sand barriers and artificial reefs are also assessed by using the surf parameter, see e.g. Atkinson et al. (2017) for a review and summary of wave runup formulae. The surf parameter is defined mostly in terms of individual wave parameters, but characteristic surf parameters are also defined in terms of sea state wave parameters (see e.g. Kim (2010); EurOtop (2018)). The surf parameter enters in many empirical formulae and theoretical models which are used to describe many of the processes referred to; relevant examples of applications are provided in e.g. Kim (2010); EurOtop (2018).

Previous works on statistical features of the surf parameter for individual waves include those of Tayfun (2006); Myrhaug and Fouques (2007, 2012); Myrhaug and Rue (2009); Myrhaug and Leira (2011); Myrhaug et al. (2016). Tayfun (2006) provided a lognormal distribution of the surf parameter, while Myrhaug and Fouques (2007) gave a combined Frèchet and lognormal distribution. Myrhaug and Fouques (2012) presented a joint distribution of wave height and surf parameter and applied it to estimate the probability of occurrence of breaking waves on slopes. The statistical features of two successive surf parameters were studied by Myrhaug and Rue (2009) as well as by Myrhaug and Leira (2011). Myrhaug et al. (2016) presented a comparative study of joint distribution of wave height and surf parameter including finite bandwidth effects. Statistical aspects of the spectral surf parameter were addressed in Myrhaug and Fouques (2010) by providing a joint distribution of significant wave height and spectral surf parameter. Recently, Myrhaug (2020) presented some probabilistic properties of

the surf parameter for individual waves and the spectral surf parameter. Furthermore, statistical properties of the spectral surf parameter were used by Myrhaug (2015); Myrhaug and Leira (2017); Myrhaug and Sunde (2018, 2019) to assess wave runup and wave rundown by adopting some of the formulae reviewed by Atkinson et al. (2017). In particular, Myrhaug (2015) and Myrhaug and Leira (2017) based their results on applying the de la Pena et al. (2014) wave runup formulae and the Blenkinsopp et al. (2016) wave runup and wave rundown formulae, respectively. Myrhaug and Sunde (2018, 2019) based their results on applying runup rundown formulae, together with long-term wind statistics (2018) and long-term wave statistics (2019).

The recent years´ research on these issues is due to the impact of climate change induced by global warming and consequences for the coastal vulnerability. For shorelines and coastal structures it is therefore crucial to be able to make reliable assessments of coastal vulnerability for safe and cost-efficient coastal protections. In this context statistical features of the surf parameter jointly with other wave characteristics are an important building stone.

Some early works of Roos and Battjes (1974), Bruun and Günbak (1977) as well as Sawaragi et al. (1982) addressed the relationship between the surf parameter, the wave runup time and the wave period, and how this is related to the stability of rubble-mound breakwaters. Thus, motivated by this the joint distributions of the surf parameter and the wave period as well as the joint distribution of wave runup time and wave period are provided here including comparison with some results from small-scale laboratory experiment by Sawaragi et al. (1982). To our knowledge these joint distributions are not available in the open literature.

The article is organized as follows. The introduction is followed by Section 2 giving the background by defining the key wave parameters and the corresponding normalized variables. Section 3 provides a comparative study of the joint distribution of surf parameter and wave period by first presenting the results of transforming the Myrhaug and Kjeldsen (1984) joint distribution of wave height and wave period (Section 3.1), as well as transforming the Longuet-

Higgins (1983) joint distribution of wave height and wave period (Section 3.2); then, these transformed distributions are compared (Section 3.3). Thus, Section 3 is essentially a comparison between the transformed theoretical Longuet-Higgins (1983) distribution and data, since the transformed Myrhaug and Kjeldsen (1984) distribution originates from a best fit to field data which are relatively broad-banded. In the remaining part of this article the Longuet-Higgins (1983) distribution of wave height and wave period is used since it contains the spectral bandwidth parameter. Section 4 provides the joint distribution of surf parameter with wave height and the joint distribution of surf parameter with wave period (Section 4.1), and how these distributions are affected by the spectral bandwidth (Section 4.2). Section 5 gives the joint distribution of wave runup time and wave period including the effect of spectral bandwidth. Section 6 makes comparison with measurements from Sawaragi et al. (1982) and predictions by using the present statistical results. Finally, a summary and the main conclusions are provided in Section 7.

2. Background

The surf parameter is defined in terms of the deep water wave conditions as $\xi = m/\sqrt{H/\lambda}$

where $m = tan\,\theta$ is the slope with an angle θ relative to the horizontal, H is the deep water wave height, $\lambda = (g/2\pi)T^2$ is the deep water wave length, T is the wave period, and g is the acceleration due to gravity. The surf parameter is normalized, i.e. $\hat{\xi} = \xi/\xi_{rms}$,where

$$\xi_{rms} = \frac{m}{[H_{rms}/((g/2\pi)T_1^2)]^{\frac{1}{2}}} \tag{1}$$

Here H_{rms} and T_1 are given in Eqs. (A2) and (A3), respectively, in Appendix A. Further, from the definition of ξ and by using Eq. (1) it follows that

$$\hat{\xi} = th^{-\frac{1}{2}} \tag{2}$$

where $h = H/H_{rms}$ and $t = T/T_1$ are the dimensionless wave height and dimensionless wave period given in Eqs. (A2) and (A3), respectively.

Roos and Battjes (1974) performed laboratory experiments on wave runup and found the following relationship between the runup time t_u, the wave period *T* and the surf parameter ξ:

$$t_u = 0.7\xi^{-\frac{1}{2}}T \tag{3}$$

Bruun and Günbak (1977) defined the so called "resonance phenomenon" related to the stability of rubble-mound breakwaters exposed to regular waves as "the condition that occurs when run-down is in a low position and wave breaking takes place simultaneously and repeatedly close to that location". Sawaragi et al. (1982) adopted this concept of resonance (see Section 6 for further details), and for irregular waves they found that the runup/rundown period to the wave period ratio was in a narrow range close to one at the same time as the surf parameter was in the range 2 to 3. More specifically, they found that resonance occurred for $2t_u/T$ in the range 0.95 to 1.0 and in the range 0.8 to 1.0 for smooth and rough impermeable slopes, respectively. It should be noted that here t_u and *T* refer to irregular waves.

Thus, by adopting Eq. (3) to be valid for irregular waves, the runup time is made dimensionless, i.e. $\hat{t}_u = t_u/t_{urms}$, where

$$t_{urms} = 0.7\xi_{rms}^{-\frac{1}{2}}T_1 \tag{4}$$

and ξ_{rms} is given in Eq. (1). By combining Eqs. (3) and (4) it follows that $\hat{t}_u = \hat{\xi}^{-\frac{1}{2}}t$, which combined with Eq. (2) gives

$$\hat{t}_u = t^{\frac{1}{2}}h^{\frac{1}{4}} \tag{5}$$

3. Comparison between joint *pdfs* of surf parameter and wave period

Here the transformed Myrhaug and Kjeldsen (1984) (hereafter referred to as MK84) joint *pdf* of wave height and wave period will be compared with the transformed Longuet-Higgins (1983) (hereafter referred to as LH83) joint *pdf* of wave height and wave period.

3.1 Transformed MK84 distribution

The MK84 joint *pdf* of h_{MK} and t_{MK} given in Appendix B is transformed to the joint *pdf* of $\hat{\xi}_{MK}$ and t_{MK} . Here $\hat{\xi}_{MK} = \xi/\bar{\xi}$, $\bar{\xi} = m[H_{rms}^1/((g/2\pi)T_{rms}^2)]^{-\frac{1}{2}}$ and ξ is the surf parameter defined in Section 2. Then, by using Eqs. (B7) and (B8) in Appendix B

$$\hat{\xi}_{MK} = t_{MK} h_{MK}^{-\frac{1}{2}} \tag{6}$$

and

$$\bar{\xi} = 1.47\xi_s;\ \xi_s = m[H_s/((g/2\pi)T_z^2)]^{-\frac{1}{2}} \tag{7}$$

where H_s and T_z are defined in Appendix B.

The joint *pdf* of $\hat{\xi}_{MK}$ and t_{MK} is obtained by a change of variables from (h_{MK}, t_{MK}) to $(\hat{\xi}_{MK}, t_{MK})$ from Eq.(B1) as (by using from Eq. (6) the Jacobian $\left|\partial h_{MK}/\partial \hat{\xi}_{MK}\right| = 2t_{MK}^2 \hat{\xi}_{MK}^{-3}$)

$$p(\hat{\xi}_{MK}, t_{MK}) = p(t_{MK}|h_{MK} = t_{MK}^2 \hat{\xi}_{MK}^{-2}) p(\hat{\xi}_{MK}; t_{MK}) \tag{8}$$

where

$$p(\hat{\xi}_{MK}; t_{MK}) = p(h_{MK} = t_{MK}^2 \hat{\xi}_{MK}^{-2}) \cdot 2t_{MK}^2 \hat{\xi}_{MK}^{-3} \tag{9}$$

It should be noted that the notation in Eq. (9) is used to make it clear that $p(\hat{\xi}_{MK}; t_{MK})$ depends explicitly on t_{MK}. By substitution in Eq. (B2), it follows that Eq. (8) can be rearranged to the Fisher-Trippett type II (Fréchet) *pdf* (Ghiocel and Lungu, 1975)

$$p(\hat{\xi}_{MK}; t_{MK}) = \kappa w^{\kappa} \hat{\xi}_{MK}^{-(\kappa+1)} \, exp\left[-(\frac{\hat{\xi}_{MK}}{w})^{-\kappa}\right]; \hat{\xi}_{MK} \geq 0 \tag{10}$$

with the scale $(w > 0)$ and the shape $(\kappa > 0)$ parameters

$$w = \hat{t}/\sqrt{1.05} \tag{11}$$

$$\kappa = 2 \cdot 2.39 \tag{12}$$

Moreover, $p(t_{MK}|h_{MK} = t_{MK}^2 \hat{\xi}_{MK}^{-2})$ is given by Eqs. (B3) to (B6) by substituting for h_{MK} , i.e. $h_{MK} = t_{MK}^2 \hat{\xi}_{MK}^{-2}$.

3.2 Transformed LH83 distribution

For comparative purposes $p(h, t)$ in Eq. (A1) in Appendix A is transformed to $p(\hat{\xi}_{MK}, t_{MK})$. This transformation affects both h versus $\hat{\xi}_{MK}$ and t versus t_{MK}, since $h = 1.01 t_{MK}^2 \hat{\xi}_{MK}^{-2}$ and $t = 1.2416(\nu^2 + 1)^{-\frac{1}{2}} t_{MK}$, respectively. Thus, the joint pdf of $\hat{\xi}_{MK}$ and t_{MK} is obtained from Eq. (A1) as (by using the Jacobian $\left|(\partial h/\partial \hat{\xi}_{MK}) \cdot (\partial t/\partial t_{MK})\right| = 2 \cdot 1.01 \cdot 1.2416(\nu^2 + 1)^{-\frac{1}{2}} t_{MK}^2 \hat{\xi}_{MK}^{-3}$)

$$p(\hat{\xi}_{MK}, t_{MK}) = \frac{3.32 L(\nu)}{\nu\sqrt{\pi}(\nu^2+1)^{-1/2}} \frac{t_{MK}^4}{\hat{\xi}_{MK}^7} \cdot exp\left\{-1.02(\frac{t_{MK}}{\hat{\xi}_{MK}})^4 \left[1 + \frac{1}{\nu^2}(1 - \frac{(\nu^2+1)^{1/2}}{1.2416 t_{MK}})^2\right]\right\} \tag{13}$$

3.3 Comparison between transformed LH83 and transformed MK84 distributions

Fig. 1 shows the isocontours of $p(\hat{\xi}_{MK}, t_{MK})$ according to Eq. (13) based on the transformed LH83 *pdf* (Fig. 1(a)), and according to Eqs. (8) to (10) based on the transformed MK84 *pdf* (Fig. 1(b)). The results for the transformed LH83 *pdf* are given for $\nu = 0.504$ corresponding to the value of the wave data upon which the MK84 parametric model is based. The peak values and their locations are given in the figure captions. It appears that the

transformed LH83 *pdf* has a peak value which is slightly higher than those for the transformed MK84 *pdf*, and located at lower t_{MK} and $\hat{\xi}_{MK}$ values than those for the transformed MK84 *pdf*. Furthermore, the transformed LH83 *pdf* extends to larger t_{MK} and $\hat{\xi}_{MK}$ values than the transformed MK84 *pdf*.

Fig 2. Shows the marginal *pdfs* of $\hat{\xi}_{MK}$ (Fig. 2(a)) and t_{MK} (Fig. 2(b)) (based on integrating the joint *pdfs* of $\hat{\xi}_{MK}$ and t_{MK} over t_{MK} and $\hat{\xi}_{MK}$, respectively) for the transformed MK84 and LH83 *pdfs*. The transformed LH83 *pdfs* give higher peak values which are shifted to the right compared with the transformed MK84 *pdfs* for both $\hat{\xi}_{MK}$ and t_{MK} .

Fig. 3 shows the conditional cumulative distribution functions (*cdfs*) of $\hat{\xi}_{MK}$ given t_{MK} in Weibull scale for $t_{MK} = 0.5, 1, 1.4, 2.1$ for the transformed LH83 (Fig. 3(a)) and MK84 (Fig. 3(b)) *pdfs*. These results are obtained by using that $p(\hat{\xi}_{MK}|t_{MK}) = p(\hat{\xi}_{MK}, t_{MK})/p(t_{MK})$. From Fig. 3(a) it is observed that for a given value of $\hat{\xi}_{MK}$ the conditional *cdf* decreases as t_{MK} increases. Further, the curves for $t_{MK} = 0.5, 1, 1.4$ are quite close for the two models, while the curves for $t_{MK} = 2.1$ are different, reflecting the different features of the transformed LH83 and MK84 *pdfs* in Fig. 1, particularly for the higher values of t_{MK}.

This section is basically a comparison between the transformed theoretical LH83 *pdf* and data, since the transformed MK84 *pdf* is originating from a best fit to field data which are relatively broad-banded. As observed in Figs. 1 to 3, it appears that the agreement between these two *pdfs* is not especially good. This is also consistent with results from previous studies including comparison between data and joint distributions of *H* and *T* (Myrhaug and Kvålsvold, 1995), as well as with the results in Myrhaug et al. (2016) who compared the transformed LH83 joint *pdf* of *H* and *T* with the Myrhaug and Fouques (2012) joint *pdf* of ξ and *H* based on the same data as the MK84 joint *pdf* of *H* and *T* (see Myrhaug and Fouques (2012) for further details). Overall, this also agrees with the results by Srokosz and Challenor (1987) who found

that the LH83 distribution gave reasonable agreement with observed wave data for $\nu < 0.4$, but poorer for $\nu > 0.5$, suggesting that the LH83 distribution is an adequate model for the joint *pdf* of H and T in the narrow-band case.

4. Joint distributions of surf parameter with wave height and wave period

In the remaining part of this article the LH83 *pdf* of *h* and *t* will be used since it contains the bandwidth effects and that it is an adequate model for $\nu < 0.4$. Thus, for the sake of completeness the LH83 *pdf* of *h* and *t* is transformed to the joint *pdfs* of $\hat{\xi}$ and h (Section 4.1) as well as $\hat{\xi}$ and *t* (Section 4.1). Effects of the spectral bandwidth are provided in Section 4.2, presenting results for ν in the range 0.1 to 0.6, i.e. in the same range as in LH83 (see Appendix A).

4.1 Joint distributions of $\hat{\xi}, h$ and $\hat{\xi}, t$

First, the LH83 joint *pdf* of *h* and *t* is transformed to the joint *pdf* of $\hat{\xi}$ and *h*, which is obtained from Eq. (A1) by a change of variables from (h, t) to $(\hat{\xi}, h)$ as (by using the Jacobian $\left|\partial t/\partial \hat{\xi}\right| = h^{\frac{1}{2}}$; see Eq. (2))

$$p(\hat{\xi}, h) = \frac{2L(\nu)}{\nu\sqrt{\pi}} \frac{h^{\frac{3}{2}}}{\hat{\xi}^2} exp\left\{-h^2\left[1 + \frac{1}{\nu^2}(1 - \frac{1}{\hat{\xi}h^{\frac{1}{2}}})^2\right]\right\} \tag{14}$$

Second, the LH83 joint *pdf* of *h* and *t* is transformed to the joint *pdf* of $\hat{\xi}$ and *t*, which is obtained from Eq. (A1) by a change of variables from (*h*, *t*) to $(\hat{\xi}, t)$ as (by using the Jacobian $\left|\partial h/\partial \hat{\xi}\right| = 2t^2\hat{\xi}^{-3}$; see Eq. (2))

$$p(\hat{\xi},t)=\frac{4L(\nu)}{\nu\sqrt{\pi}}\frac{t^4}{\hat{\xi}^7}exp\left\{-(\frac{t}{\hat{\xi}})^4\left[1+\frac{1}{\nu^2}(1-\frac{1}{t})^2\right]\right\} \quad (15)$$

4.2 Effects of spectral bandwidth

Fig. 4 shows the marginal *pdfs* of $\hat{\xi}$ (Fig. 4(a)), h (Fig. 4(b)) and t (Fig. (4 (c)) (i.e. based on integrating the joint *pdfs* over the other variable) for $\nu = 0.1, 0.3, 0.5, 0.6$. From Fig. 4(a) it appears that $p(\hat{\xi})$ is sensitive to the variation of ν; the peak value is shifted to lower values of $\hat{\xi}$ with a lower peak value as ν increases. From Fig. 4(b) it appears that $p(h)$ is only slightly sensitive to the variation of ν; the peak value is shifted slightly to higher values of h with a slightly higher peak value as ν increases. From Fig. 4(c) it appears that $p(t)$ is very sensitive to the variation of ν; the peak value is shifted to lower values of t with a lower peak value as ν increases. Thus, it appears that the features of $p(t)$ dominate the features of $p(\hat{\xi})$.

Fig. 5 shows the isocontours of $p(\hat{\xi},h)$ according to Eq. (14) for $\nu = 0.1, 0.3, 0.5, 0.6$. The peak values and their locations are given in Table 1. It appears that the *pdf* becomes wider as ν increases (Fig. 5(a) to (d)), and accordingly the peak values decrease from 4.3 to 1.0 as ν increases; the location of the peak value is also slightly shifted towards lower $(\hat{\xi},h)$ values as ν increases (Table 1). Overall, these features reflect that the sea state contains a wider range of wave periods as the spectral bandwidth increases. These features are also similar and consistent with those shown in Fig. 1 in Myrhaug et al. (2016).

Fig. 6 shows the conditional *cdf* of $\hat{\xi}$ given h versus $\hat{\xi}$ in Weibull scale for $\nu = 0.5$ and $h = 0.5, 1.0, 1.4, 2.1$. This result is obtained by utilizing that $p(\hat{\xi}|h) = p(\hat{\xi},h)/p(h)$ by using the transformed LH83 *pdf* in Eq. (14) and $p(h)$ is obtained by integrating Eq. (14) over $\hat{\xi}$ (or by using $p(h)$ as given in LH83). From Fig. 6 it is observed that for a given value of $\hat{\xi}$ the conditional *cdf* increases as h increases for $\hat{\xi}$ exceeding about 0.6, or, the probability of

exceeding about $\hat{\xi} = 0.6$ decreases as *h* increases. Similar features were obtained in Myrhaug and Fouques (2012) and Myrhaug et al. (2016) (see their Fig. 4). These references also demonstrated the application of their results estimating the probability of occurrence of breaking waves on slopes by using the classification of breaking waves in terms of the surf parameter.

Fig 7 shows the isocontours of $p(\hat{\xi}, t)$ according to Eq. (15) for $\nu = 0.1, 0.3, 0.5, 0.6$. The peak values and their locations are given in Table 1. It appears that the *pdf* becomes wider as ν increases (Fig. 7(a) to (d)), and accordingly the peak values decrease from 10.6 to 2.8 as ν increases; the location of the peak value is only slightly shifted towards lower $(\hat{\xi}, t)$ values as ν increases (Table 1). As in Fig. 5, these features reflect that the sea state contains a wider range of wave periods as the spectral bandwidth increases. The results in Fig. 7(c) are similar and consistent with those shown in Fig. 1(a).

Fig. 8 shows the conditional *cdf* of $\hat{\xi}$ given *t* versus $\hat{\xi}$ in Weibull scale for $\nu = 0.5$ and $t = 0.5, 1.0, 1.4, 2.1$. This result is obtained by utilizing that $p(\hat{\xi}|t) = p(\hat{\xi}, t)/p(t)$ by using the transformed LH83 *pdf* in Eq. (15) and $p(t)$ is obtained by integrating Eq. (15) over $\hat{\xi}$ (or by using $p(t)$ as given in LH83). From Fig. 8 it is observed that the conditional *cdf* decreases as t increases. These results are similar and consistent with those shown in Fig. 3(b).

5. Joint distribution of wave runup time and wave period

The LH83 joint *pdf* of *h* and *t* is transformed to the joint *pdf* of $\hat{t}_u$ and *t*, where $\hat{t}_u$ is given in Eq. (5). Then the joint *pdf* of $\hat{t}_u$ and *t* is obtained from Eq. (A1) by a change of variables from (h, t) to $(\hat{t}_u, t)$ as (by using the Jacobian $|\partial h/\partial \hat{t}_u| = 4t^{-2}\hat{t}_u^3$; see Eq. (5))

$$p(\hat{t}_u, t) = \frac{8L(\nu)}{\nu\sqrt{\pi}} \frac{\hat{t}_u^{11}}{t^8} exp\left\{-\frac{\hat{t}_u^8}{t^4}\left[1 + \frac{1}{\nu^2}(1 - \frac{1}{t})^2\right]\right\} \quad (16)$$

Fig. 9 shows the isocontours of $p(\hat{t}_u, t)$ according to Eq. (16) for $\nu = 0.1, 0.3, 0.5, 0.6$. The peak values and their locations are given in Table 1. It appears that the *pdf* becomes wider as ν increases (Fig. 9(a) to (d), and accordingly the peak values decrease from 17.9 to 4.5 as ν increases; the location of the peak value is only shifted slightly towards lower $(\hat{t}_u, t)$ values as ν increases. These features also reflect that the sea state contains a wider range of wave periods as the spectral bandwidth increases. However, for a given value of ν, $p(\hat{t}_u, t)$ is narrower than $p(\hat{\xi}, t)$ which is mainly due to that $\hat{t}_u$ has a weaker dependence on t than $\hat{\xi}$ has; see Eq. (5) and Eq. (2), respectively.

Fig. 10 shows the marginal *pdf* of $\hat{t}_u$ based on integrating Eq. (16) over *t* for $\nu = 0.1, 0.3, 0.5, 0.6$. From Fig. 10 it appears that $p(\hat{t}_u)$ is sensitive to the variation of ν; the peak value decreases as ν increases; the location of the peak value is slightly sensitive to the variation in ν. It appears that the location of the peak value increases slightly as ν decreases from 0.6 to 0.3, and then it decreases slightly as ν decreases from 0.3 to 0.1. Thus, it appears that the features of $p(t)$ dominates the features of $p(\hat{t}_u)$.

Fig. 11 shows the conditional *cdf* of $\hat{t}_u$ given *t* versus $\hat{t}_u$ in Weibull scale for $\nu = 0.5$ and $t = 0.5, 1.0, 1.4, 2.1$. This result is obtained utilizing that $p(\hat{t}_u|t) = p(\hat{t}_u, t)/p(t)$ by using the transformed LH83 *pdf* in Eq. (16) and $p(t)$ is obtained by integrating Eq. (16) over $\hat{t}_u$ (or by using $p(t)$ as given in LH83). From Fig. 11 it is observed that for a given value of $\hat{t}_u$ the conditional *cdf* decreases as *t* increases. To the authors´ knowledge no data exist to compare with. However, based on the previous comparison of $p(\hat{\xi}, h)$ and now with $p(\hat{\xi}, t)$, this should give some confidence that $p(\hat{t}_u, t)$ is reasonable.

6. Comparison with experiments

Sawaragi et al. (1982) provided results from small-scale laboratory experiments on the condition of resonance and the probability of occurrence of resonance (as referred to in Section 2) on steep slopes of coastal structures for regular and irregular waves. Here comparison will be made with the six cases for irregular waves. Random waves were generated by a Bretschneider spectrum for which $\nu = 0.42$ (Tucker and Pitt, 2001) over an impermeable smooth surface with a slope of $\theta = 30$ degrees. The wave conditions are given in Table 2 for tests W1 – W6, representing waves with H_s in the range 0.030 m to 0.055 m and T_1 in the range 0.75 s to 0.97 s giving ξ_{rms} in the range 3.1 to 4.8 (by using that $H_{rms} = H_s/\sqrt{2}$ based on that *H* is Rayleigh-distributed (Tucker and Pitt, 2001). As referred to in Section 3.3 the LH83 *pdf* is an adequate model for the *H, T* distribution for $\nu < 0.4$. Thus, the present results based on the LH83 *pdf* for $\nu = 0.42$ should be close enough to be considered as acceptable.

First, Fig. 12 shows that the *pdf* of ξ for test W5 represented by the histogram and the present model (i.e. obtained from Eq. (14) by integrating over *h*). It appears to be a fair agreement between the model and the data.

Second, as referred to in Section 2, resonance occurred simultaneously with that $2 \leq \xi \leq 3$, where the probability of this to occur is obtained as

$$Prob(2 \leq \xi \leq 3) = \int_0^\infty \int_{2/\xi_{rms}}^{3/\xi_{rms}} p(\hat{\xi}, h) d\hat{\xi} dh \tag{17}$$

where $p(\hat{\xi}, h)$ is given in Eq. (14). The results are given in Table 2 together with those obtained from the measurements, showing good agreement for all test cases.

Finally, the probability of resonance is calculated by multiplying the result in Eq. (17) with the probability of $0.8 \leq 2t_u/T \leq 1.0$ (i.e. for rough impermeable slopes as referred to in Section 2) obtained as

$$Prob(0.4T \leq t_u \leq 0.5T) = \int_0^{\infty} \int_{\hat{t}_{u1}}^{\hat{t}_{u2}} p(\hat{t}_u, t) d\hat{t}_u dt \quad (18)$$

where $\hat{t}_{u1} = 0.57\sqrt{\xi_{rms}}t$ and $\hat{t}_{u2} = 0.71\sqrt{\xi_{rms}}t$. Overall, it appears that the predicted values obtained by multiplying the results in Eqs. (17) and (18) are larger than those obtained from the measurements. However, the agreement is good for test W5.

It should be noticed that strictly the integral in Eq. (18) should be evaluated for the case corresponding to $0.95 \leq 2t_u/T \leq 1.0$ for smooth impermeable slopes, and not for rough impermeable slopes (see Section 2). However, by using this range of $2t_u/T$, the probability of resonance becomes too small compared with those from the measurements, i.e. the predicted values for the tests W2 to W6 are in the range 0.0012 to 0.0073. Thus, the predicted results for resonance given in Table 2 cover resonance and semi-resonance for smooth and rough impermeable slopes.

7. Summary and conclusions

A summary and the main conclusion are as follows.

Results from revisiting joint distributions of surf parameter with characteristic wave parameters for individual random waves including spectral bandwidth effects are presented.

First, results from a comparative study of the joint distribution of surf parameter and wave period are provided. The transformed Myrhaug and Kjeldsen (1984) joint distribution of wave height and wave period is compared with the transformed Longuet-Higgins (1983) joint distribution of wave height and wave period. The Myrhaug and Kjeldsen (1984) distribution is a parametric model originating from a best fit to relatively broad-band field data, whilst the Longuet-Higgins (1983) distribution is theoretically based. Thus, this is essentially a comparison between the transformed Longuet-Higgins distribution and data. It appears that the

theoretically based distribution does not represent the features of the parametric model especially well, suggesting that parametric models should be used to describe relatively broad-banded data.

Second, in order to study the effects of the spectral bandwidth the Longuet-Higgins (1983) distribution is transformed to the joint distribution of surf parameter with wave height and wave period. It is demonstrated how that the statistical features of these joint distributions are affected by the spectral bandwidth.

Third, the Longuet-Higgins (1983) distribution is transformed to the joint distribution of wave runup time and wave period due to its relation to the stability of rubble-mound breakwaters. Comparisons are made with statistical results obtained by Sawaragi et al. (1982) who performed small-scale laboratory experiments addressing issues related to stability of rubble-mound breakwaters. The present results agree well with the distribution of the surf parameter, whilst the agreement is poorer between predictions and measurements for the probability of resonance.

Appendix A. LH83 distribution

The LH83 joint *pdf* of wave height and wave period is based on the statistics of the wave envelope, i.e. the joint *pdf* of the envelope amplitude and the time derivative of the envelope phase. It is also based on the narrow-band approximation, and is given as

$$p(h,t) = \frac{2L(\nu)}{\nu\sqrt{\pi}} \left(\frac{h}{t}\right)^2 exp\left\{-h^2\left[1+\frac{1}{\nu^2}\left(1-\frac{1}{t}\right)^2\right]\right\} \quad \text{(A1)}$$

where

$$h = \frac{H}{H_{rms}}; H_{rms} = 2\sqrt{2m_0} \quad \text{(A2)}$$

$$t = \frac{T}{T_1}; T_1 = 2\pi \frac{m_0}{m_1} \tag{A3}$$

are dimensionless wave height and wave period in deep water, respectively, and

$$L(\nu) = \frac{2}{1+(1+\nu^2)^{-\frac{1}{2}}} \tag{A4}$$

$$\nu^2 = \frac{m_0 m_2}{{m_1}^2} - 1 \tag{A5}$$

Here m_n is the spectral moments defined as

$$m_n = \int_0^\infty \omega^n S(\omega) d\omega; n = 0,1,2, - - - - \tag{A6}$$

where $S(\omega)$ is the single-sided wave spectrum, and ω is the circular wave frequency. The bandwidth parameter ν is small for a narrow-band spectrum, and LH83 provided results for ν in the range 0.1 to 0.6. LH83 also presented analytical formulae for the marginal *pdf* of $h, p(h)$, and the conditional *pdf* of t given $h, p(t|h)$ (see LH83 for further details).

Appendix B. MK84 distribution

The MK84 joint *pdf* of wave height and wave period was obtained as best fit to data from wave measurements with waverider buoys made at three different deep water locations at sea on the Norwegian continental shelf. The MK84 distribution is given as

$$p(h_{MK}, t_{MK}) = p(t_{MK}|h_{MK}) p(h_{MK}) \tag{B1}$$

where the marginal *pdf* of h_{MK} is given by the two-parameter Weibull *pdf*

$$p(h_{MK}) = \frac{2.39 h_{MK}^{1.39}}{1.05^{2.39}} exp\left[-(\frac{h_{MK}}{1.05})^{2.39}\right];\ h_{MK} \geq 0 \tag{B2}$$

and the conditional *pdf* of t_{MK} given h_{MK} is given by the three-parameter Weibull *pdf*

$$p(t_{MK}|h_{MK}) = \frac{\beta}{\rho}\left(\frac{t_{MK}-\gamma}{\rho}\right)^{\beta-1} exp\left[-\left(\frac{t_{MK}-\gamma}{\rho}\right)^{\beta}\right];\ t_{MK} \geq \gamma \quad \text{(B3)}$$

with the parameters

$$\gamma = 0.12\sqrt{h_{MK}} \quad \text{(B4)}$$

$$\rho = \begin{cases} 0.78h_{MK} + 0.26 \text{ for } h_{MK} \leq 0.9 \\ 0.962 \text{ for } h_{MK} > 0.9 \end{cases} \quad \text{(B5)}$$

$$\beta = 2\, arctan[2(h_{MK} - 1.2)] + 5 \quad \text{(B6)}$$

Here

$$h_{MK} = \frac{H}{H_{rms}^1}; H_{rms}^1 = 0.714H_s \quad \text{(B7)}$$

$$t_{MK} = \frac{T}{T_{rms}}; T_{rms} = 1.2416T_z \quad \text{(B8)}$$

are dimensionless wave height and wave period in deep water, respectively, and $H_s = 4\sqrt{m_0}$ is the significant wave height and $T_z = 2\pi\sqrt{m_0/m_2}$ is the mean zero-crossing wave period (see MK84 for further details).

References

Atkinson, A. L., Power, H.E., Monra, T., Callaghan, D.P., Baldock, T.E., 2017. Assessment of runup predictions by empirical models on non-truncated beaches on the south-east Australian coast. *Coastal Engineering* 119: 15-31, https://doi.org/10.1016/j.coastaleng.2016.10.001.

Baldock, T.E., Cox, D., Maddux, K., Killian, J., Fayler, L., 2009. Kinematics of breaking tsunami wave fronts: A data set from large scale laboratory experiments. *Coastal Engineering* 56 (5-6): 506-516, https://doi.org/10.1016/j.coastaleng.2008.10.011.

Battjes, J.A., 1974. Surf similarity. *Proceedings 14th Int. Conf. on Coastal Engineering*, vol. 1. ASCE, New York, pp. 466-479.

Blenkinsopp, C.E., Matias, A., Howe, D., Castelle, B., Marieu, V., Turner, I.L., 2016. Wave runup and overwash on a prototype-scale sand barrier. *Coastal Engineering* 113: 88-103, https://doi.org/10.1016/j.coastaleng.2015.08.006.

Bruun, P., Günbak, A.R., 1977. Stability of sloping structures in relation to $\xi = tan\,\alpha\,/\sqrt{H/L_0}$ risk criteria in design. *Coastal Engineering* 1: 287-322.

de la Pena, J.M., Sanches-Gonzales, J.F., Diaz-Sanches, R., 2014. Wave runup in a sand bed physical model. *Journal of Waterways, Port, Coastal and Ocean Engineering* 140(4): 04014015-1-04014015-11, https://doi.org/10.1061/(ASCE)ww.1943-5460.0000246.

EurOtop, 2018. Manual on wave overtopping of sea defences and related structures. An overtopping manual based on European research, but for worldwide application. Van der Meer, J.W., Allsop, N.W.H., Bruce, T., De Rouck, J., Kortenhaus, A., Pullen, T., Schuttrumpf, H., Troch, P., Zanuttigh, B., www.overtopping-manual.com.

Iribarren, C.R., Nogales, C., 1949. Protection des ports (Sect. 2, Comm. 4) *17th Int. Nav. Congress*, Lisbon, pp. 31-80.

Kim, Y.C., 2010. *Handbook of Coastal and Ocean Engineering*. World Scientific, Singapore, 1163 pp.

Longuet-Higgins, M.S., 1983. On the joint distribution of wave periods and amplitudes in a random wave field. *Proc. R. Soc. London*, Ser. A 389: 241-258.

Myrhaug, D., 2015. Estimation of wave runup on shorelines based on long-term variation of wave conditions. *Journal of Ocean Engineering and Marine Energy* 1(2): 193-197, https://doi.org/10.1007/S40722-015-0016-4.

Myrhaug, D., 2020. Some probabilistic properties of surf parameter. *Oceanologia* 62, in press, https://doi.org/10.1016/j.oceano.2020.xx.xxx.

Myrhaug, D., Fouques, S., 2007. Discussion of "Distributions of wave steepness and surf parameter" by M. Aziz Tayfun. *Journal of Waterway, Port, Coastal, and Ocean Engineering* 133(3): 242-243, https://doi.org/10.1061/(ASCE)0733-950X(2007) 133:3(242).

Myrhaug, D., Fouques, S., 2010. A joint distribution of significant wave height and characteristic surf parameter. *Coastal Engineering* 57(10): 948-952, https://doi.org/10.1016/j.coastaleng. 2010.05.001.

Myrhaug, D., Fouques, S., 2012. Joint distributions of wave height with surf parameter and breaker index for individual waves. *Coastal Engineering* 60: 235-247, https://doi.org/10.1016/j.coastaleng.2011.10.008.

Myrhaug, D., Kjeldsen, S.P., 1984. Parametric modelling of joint probability density distributions for steepness and asymmetry in deep water waves. *Applied Ocean Research*, 6(4): 207-220.

Myrhaug, D., Kvålsvold, J., 1995. Comparative study of joint distributions of primary wave characteristics. *Journal of Offshore Mechanics and Arctic Engineering*, ASME, 117: 91-98.

Myrhaug, D., Leira, B.J., 2011. A bivariate Fréchet distribution and its application to the statistics of two successive surf parameters. *Proceedings Institute Mechanical Engineers, I Mech E Part M: Journal of Engineering for the Maritime Environment* 225(1): 67-74, https://doi.org/10.1243/14750902JEME205.

Myrhaug, D., Leira, B.J., 2017. Application of wave runup and wave rundown formulae based on long-term variation of wave conditions. *Coastal Engineering* 120: 75-77, https://doi.org/10.1016/j.coastaleng. 2016.11.013.

Myrhaug, D., Li, H., Wang. H., 2016. Comparative study of joint distributions of wave height and surf parameter for individual waves including spectral bandwidth effects. *Coastal Engineering* 114: 341-346, https://doi.org/10.1016/j.coastaleng.2016.05.002.

Myrhaug., D., Rue, H., 2009. On a joint distribution of two successive surf parameters. In: Brebbia, C.A., Benassai, G., Rodriquez, G., (Eds.), *Coastal Processes.* Wit Press, Southampton, Hampshire, UK, pp. 85-96.

Myrhaug, D., Sunde, T., 2018. Wave runup and wave rundown estimation based on long-term variation of wind statistics. *Proceedings of the Institution of Civil Engineers – Maritime Engineering* 171(1): 40-46, https://doi.org/10.1680/jmaen.2017.12.

Myrhaug, D., Sunde, T., 2019. Assessment of wave runup and wave rundown estimation based on observed long-term wave conditions. *IOP Conf. Series: Material Science and Engineering* 700:012006, https://doi.org/10.1088/1757-899X/700/1/012006.

Poate, T.G., McCall, R.T., Masselink, G., 2016. A new parameterization for runup on gravel beaches. *Coastal Engineering*, 117: 176-190, https://doi.org/10.1016/j.coastaleng. 2016.08.003.

Roos, A., Battjes, J.A., 1976. Characteristics of flow in runup of periodic waves. *Proceedings 15th Int. Conf. on Coastal Engineering*, Honolulu, pp. 781-795.

Sawaragi, T., Iwata, K., Kobayaski, M., 1982. Condition and probability of occurrence of resonance on steep slopes of coastal structures. *Coastal Engineering in Japan* 25: 75-90.

Srokosz, M.A., Challenor, P.G., 1987. Joint distributions of wave height and period: a critical comparison. *Ocean Engineering* 14(4): 295-311.

Tayfun, M.A., 2006. Distributions of wave steepness and surf parameter. *Journal of Waterway, Port, Coastal, and Ocean Engineering* 132(1): 1-9,

https://doi.org/10.1061/(ASCE)0733-950X(2006) 132:1(1).

Tucker, M.J., Pitt, E.G., 2001. *Waves in Ocean Engineering*. Elsevier, Amsterdam, 521 pp.

Table 1 Peak values and their locations for $p(\hat{\xi},h)$ (Eq. (14)), $p(\hat{\xi},t)$ (Eq. (15)), $p(\hat{t}_u,t)$ (Eq. (16))

Distribution	ν	$\hat{\xi}$	h	$\hat{t}_u$	t	Peak value
$p(\hat{\xi},h)$	0.1	0.94	1.11	--	--	4.32
	0.3	0.90	1.09	--	--	1.56
	0.5	0.82	1.04	--	--	1.08
	0.6	0.78	1.02	--	--	0.98
$p(\hat{\xi},t)$						
	0.1	0.86	--	--	0.99	10.60
	0.3	0.82	--	--	0.93	3.97
	0.5	0.75	--	--	0.83	2.94
	0.6	0.71	--	--	0.77	2.79
$p(\hat{t}_u,t)$						
	0.1	--	--	1.04	0.99	17.90
	0.3	--	--	0.99	0.93	6.64
	0.5	--	--	0.92	0.82	4.81
	0.6	--	-	0.88	0.76	4.50

Table 2 Comparison with measurements from Sawaragi et al. (1982)

Test No	H_s (m)	T_1 (s)	ξ_{rms}	Prob $(2 \leq \xi \leq 3)$		Prob (resonance)	
				meas	pred Eq. (17)	meas	pred Eq. (17)xEq. (18)
W1	0.0299	0.97	4.81	0.02	0.04	0	0
W2	0.0365	0.75	3.37	0.30	0.33	0.017	0.060
W3	0.0537	0.85	3.15	0.37	0.38	0.083	0.108
W4	0.0499	0.84	3.22	0.32	0.37	0.046	0.093
W5	0.544	0.83	3.05	0.40	0.40	0.115	0.122
W6	0.0499	0.80	3.07	0.39	0.40	0.094	0.115

Figure captions

Fig. 1 Isocontours of $p(\hat{\xi}_{MK}, t_{MK})$ for: (a) the transformed LH83 *pdf* for $\nu = 0.504$ with $pdf_{max} = 3.59$ for $\hat{\xi}_{MK} = 0.68$, $t_{MK} = 0.74$; (b) the transformed MK84 *pdf* with $pdf_{max} = 3.48$ for $\hat{\xi}_{MK} = 0.91$, $t_{MK} = 1.02$.

Fig. 2 Marginal *pdfs* based on the transformed LH83 *pdf* for $\nu = 0.504$ and MK84 *pdfs* for: (a) $p(\hat{\xi}_{MK})$; (b) $p(t_{MK})$.

Fig. 3 $P(\hat{\xi}_{MK}|t_{MK})$ versus $\hat{\xi}_{MK}$ in Weibull scale for: (a) the transformed LH83 *pdf* for $\nu = 0.504$ and the given values of t_{MK} ; (b) the corresponding results for the transformed MK84 *pdf*.

Fig. 4 Marginal *pdfs* based on the transformed LH83 *pdf* for $\nu = 0.1, 0.3, 0.5, 0.6$: (a) $p(\hat{\xi})$; (b) $p(h)$; (c) $p(t)$.

Fig. 5 Isocontours of the transformed LH83 $p(\hat{\xi}, h)$ for: (a) $\nu = 0.1$; (b) $\nu = 0.3$; (c) $\nu = 0.5$; (d) $\nu = 0.6$.

Fig. 6 $P(\hat{\xi}|h)$ versus $\hat{\xi}$ in Weibull scale for the transformed LH83 distribution for $\nu = 0.5$ and the given values of *h*.

Fig. 7 Isocontours of the transformed LH83 $p(\hat{\xi}, t)$ for: (a) $\nu = 0.1$; (b) $\nu = 0.3$; (c) $\nu = 0.5$; (d) $\nu = 0.6$.

Fig.8 $P(\hat{\xi}|t)$ versus $\hat{\xi}$ in Weibull scale for the transformed LH83 distribution for $\nu = 0.5$ and the given values of *t*.

Fig. 9 Isocontours of the transformed LH83 $p(\hat{t}_u, t)$ for: (a) $\nu = 0.1$; (b) $\nu = 0.3$; (c) $\nu = 0.5$; (d) $\nu = 0.6$.

Fig. 10. $p(\hat{t}_u)$ based on the transformed LH83 distribution for $\nu = 0.1, 0.3, 0.5, 0.6$.

Fig. 11 $P(\hat{t}_u|t)$ versus $\hat{t}_u$ in Weibull scale for the transformed LH83 distribution for $\nu = 0.5$ and the given values of *t*.

Fig. 12 Measured and predicted $p(\xi)$; the histogram represents test W5 from Sawaragi et al. (1982); the curve represents the transformed LH83 distribution for $\nu = 0.42$.

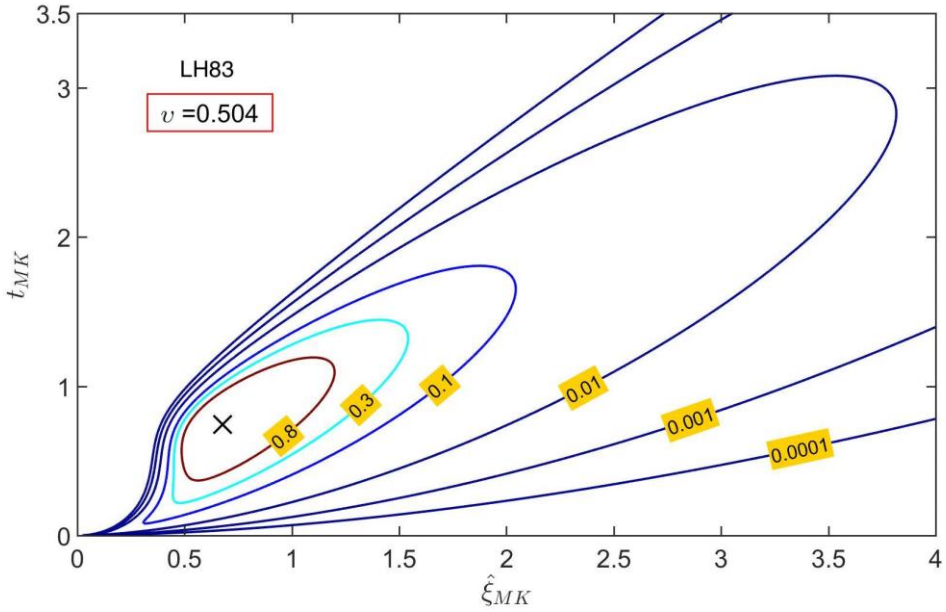

Figure 1(a)

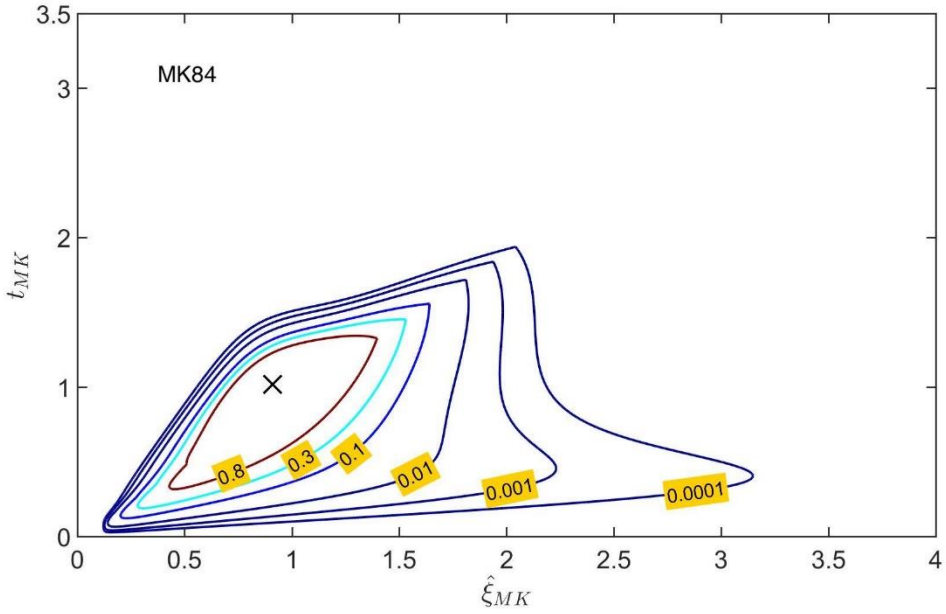

Figure 1(b)

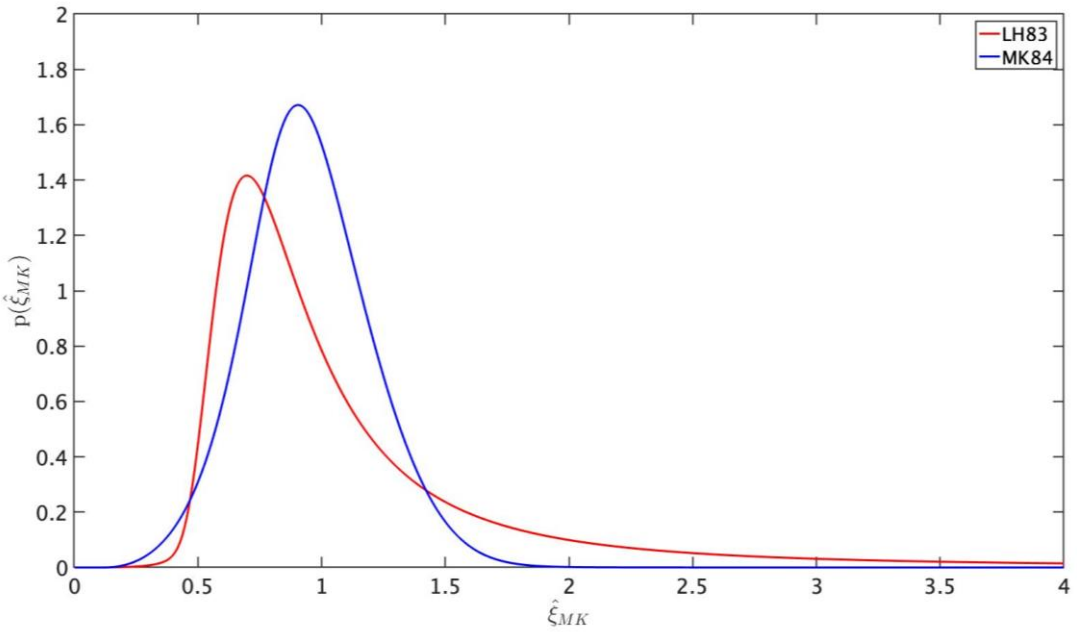

Figure 2(a)

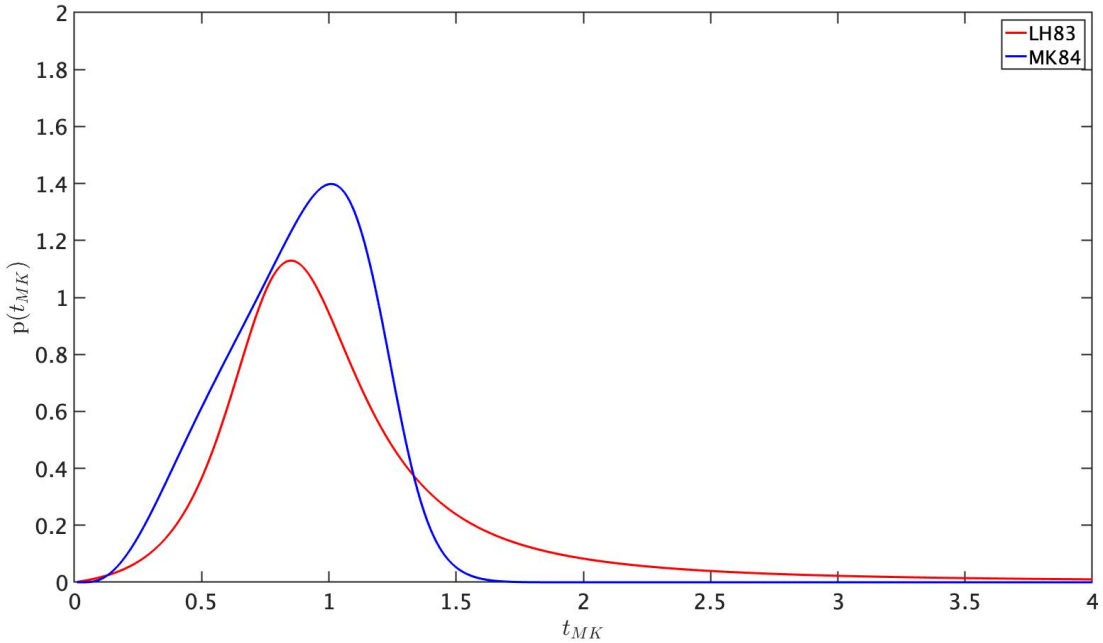

Figure 2(b)

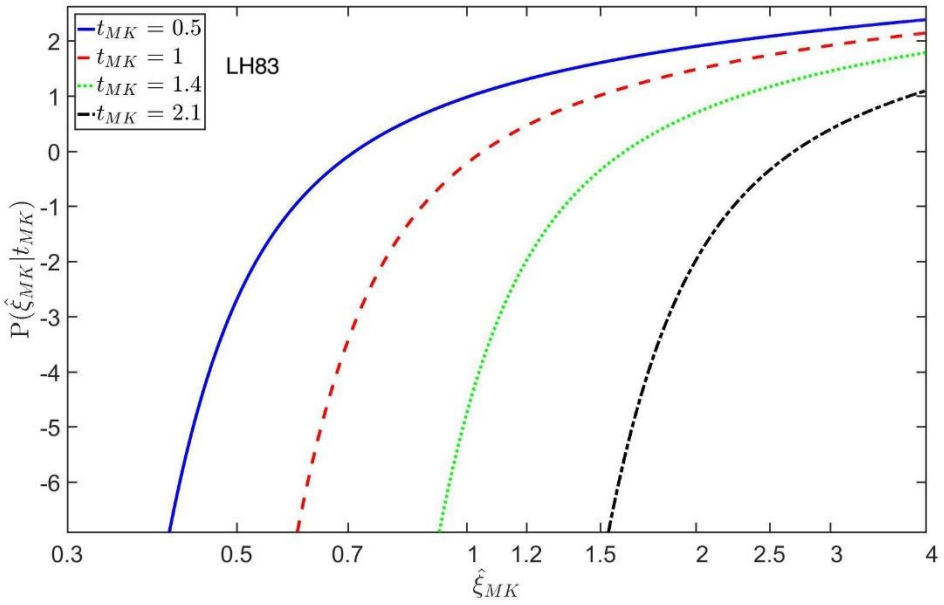

Figure 3(a)

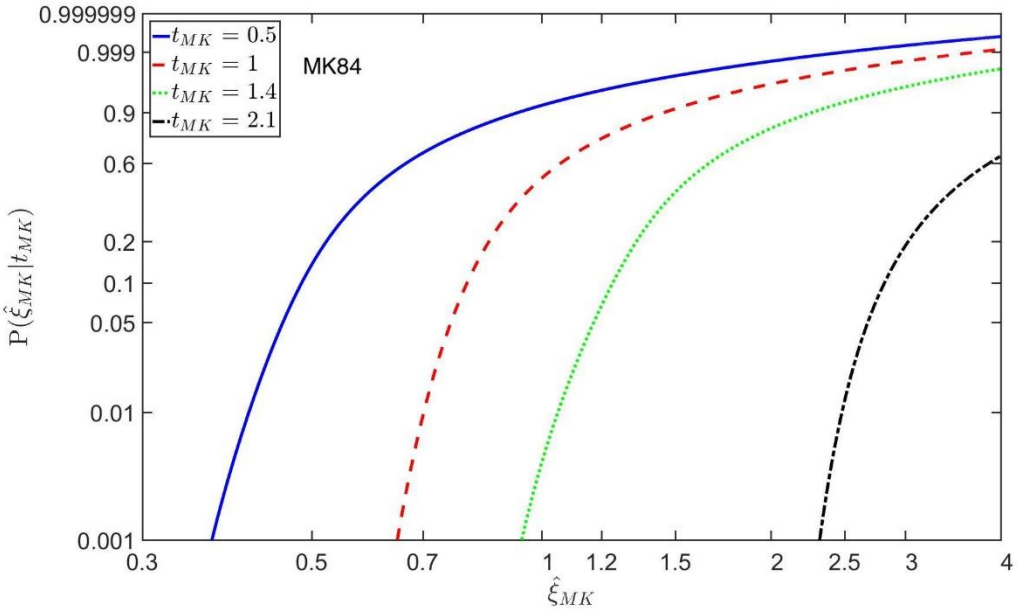

Figure 3(b)

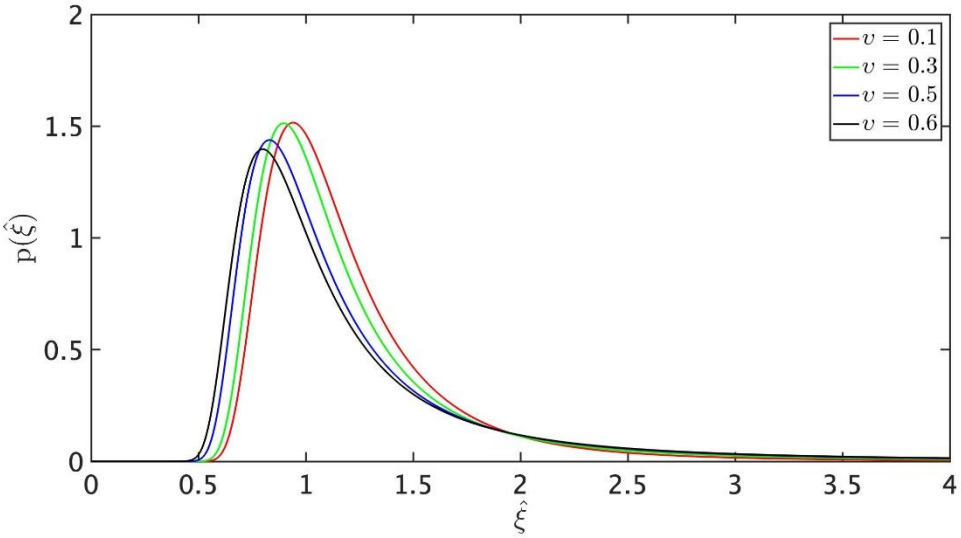

Figure 4(a)

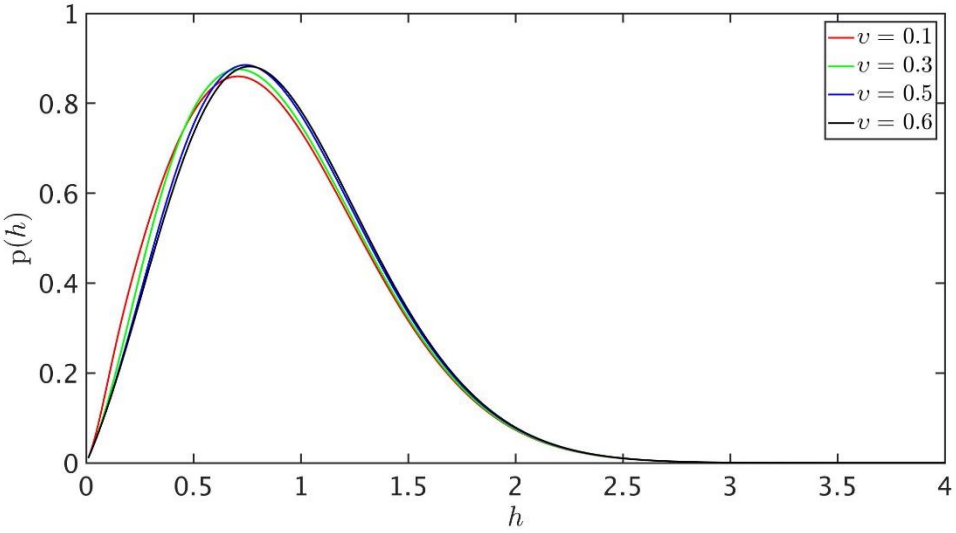

Figure 4(b)

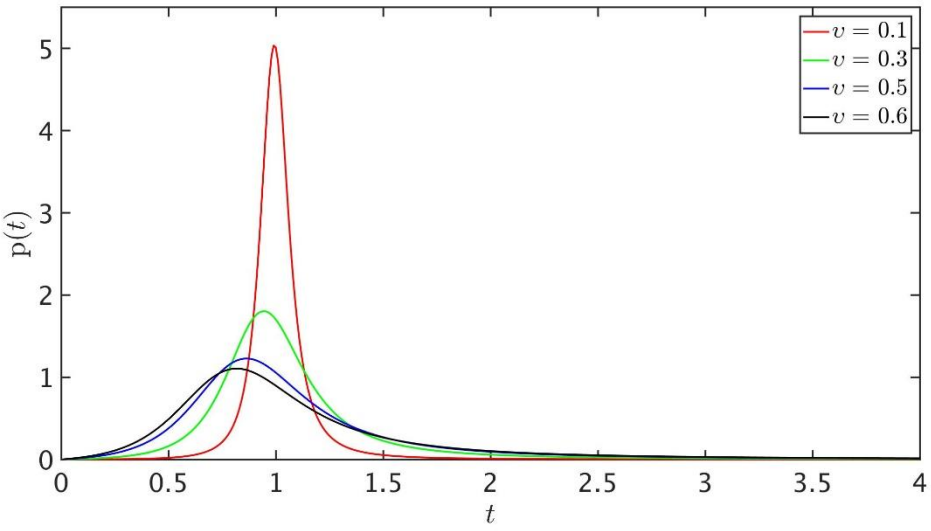

Figure 4(c)

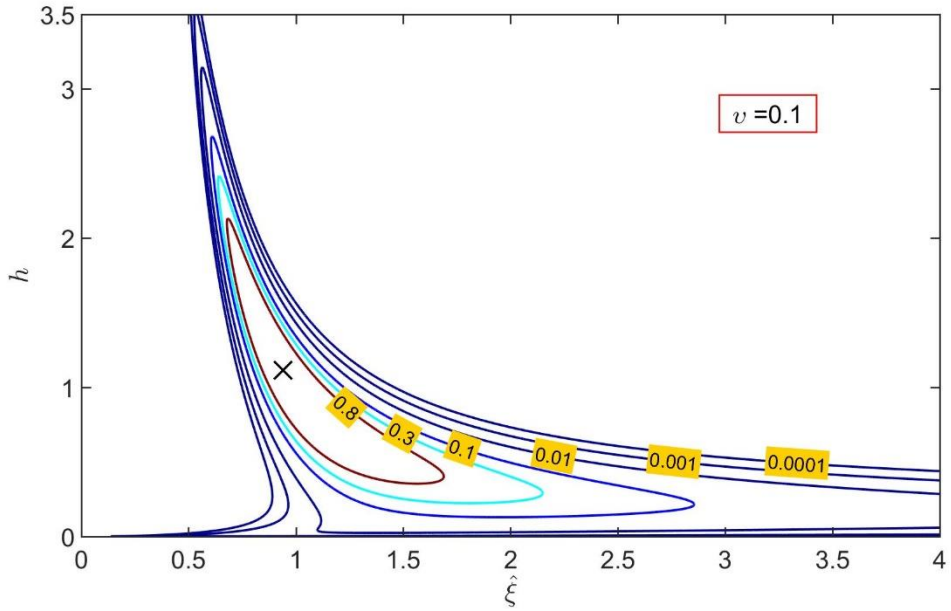

Figure 5(a)

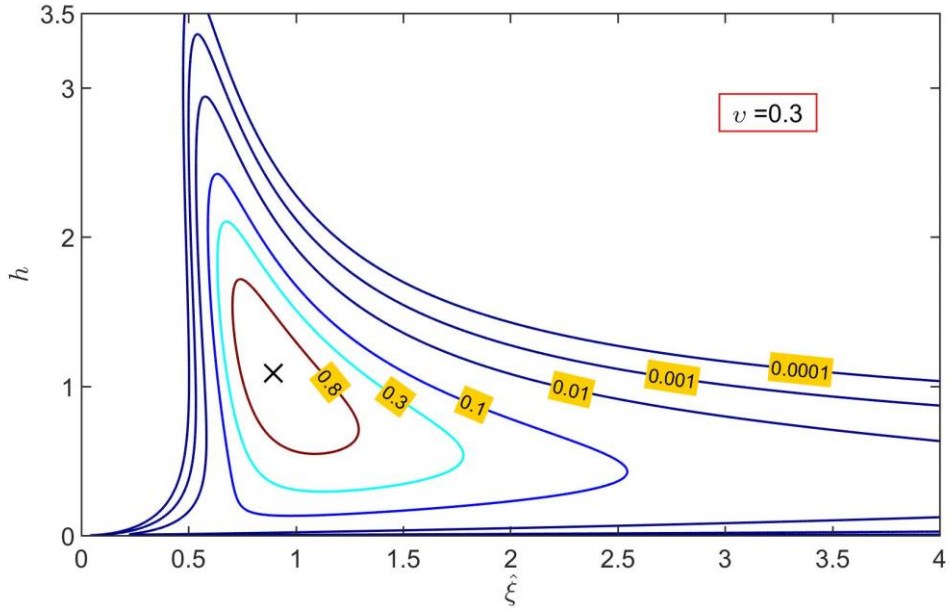

Figure 5(b)

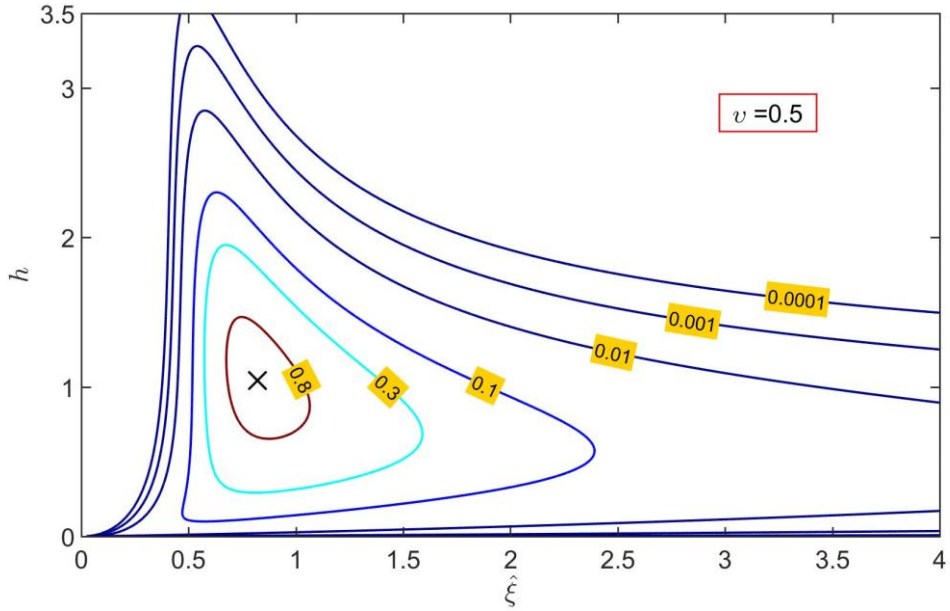

Figure 5(c)

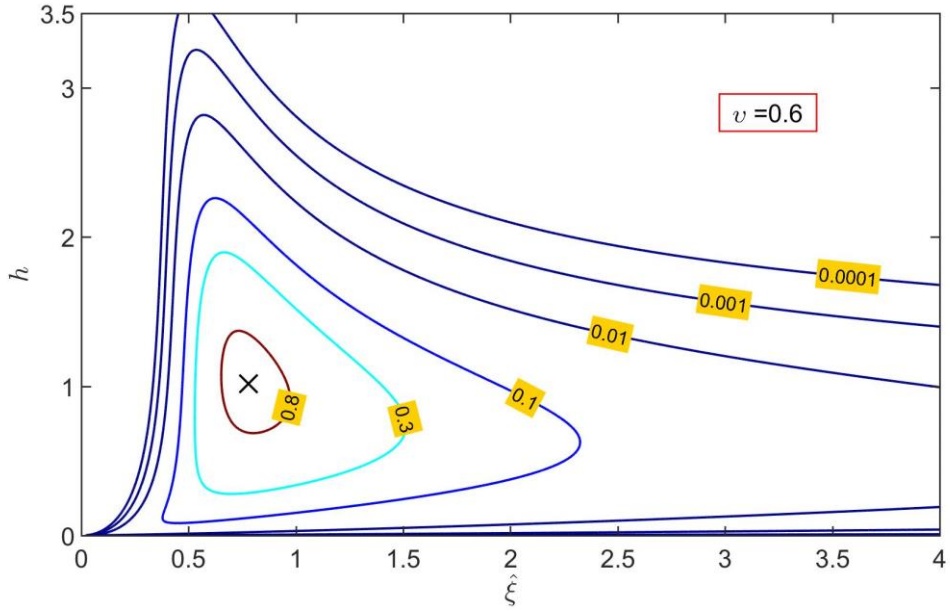

Figure 5(d)

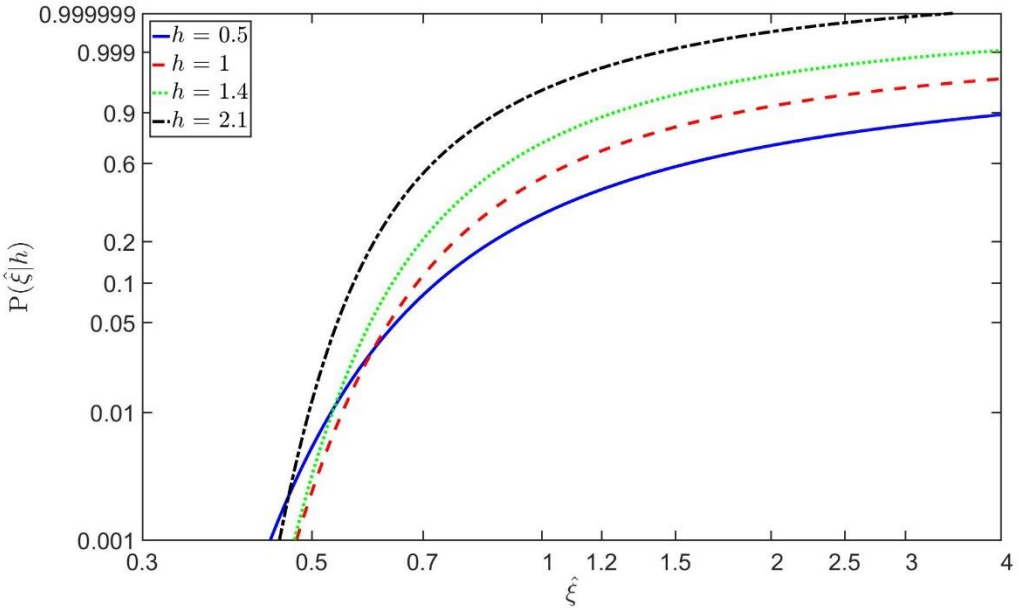

Figure 6

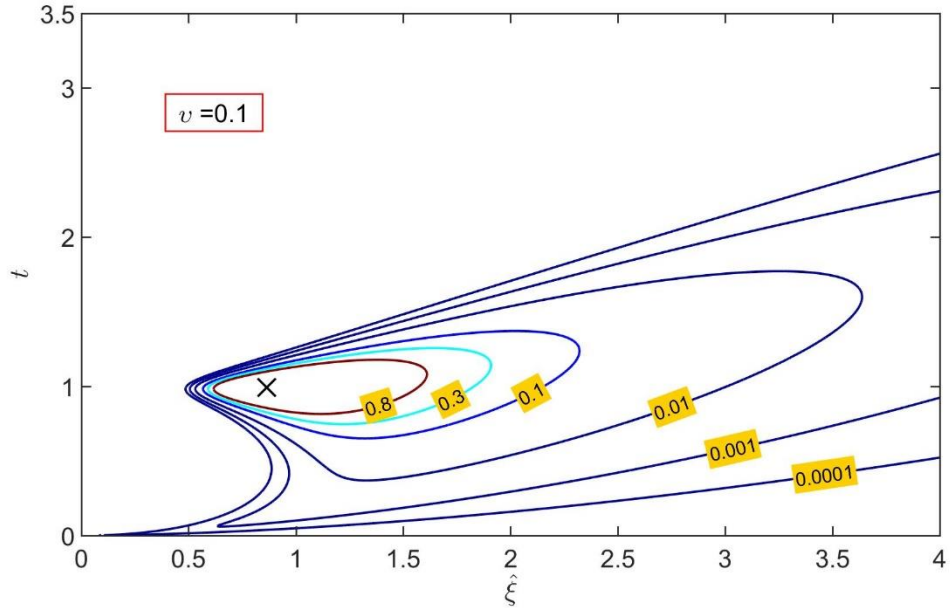

Figure 7(a)

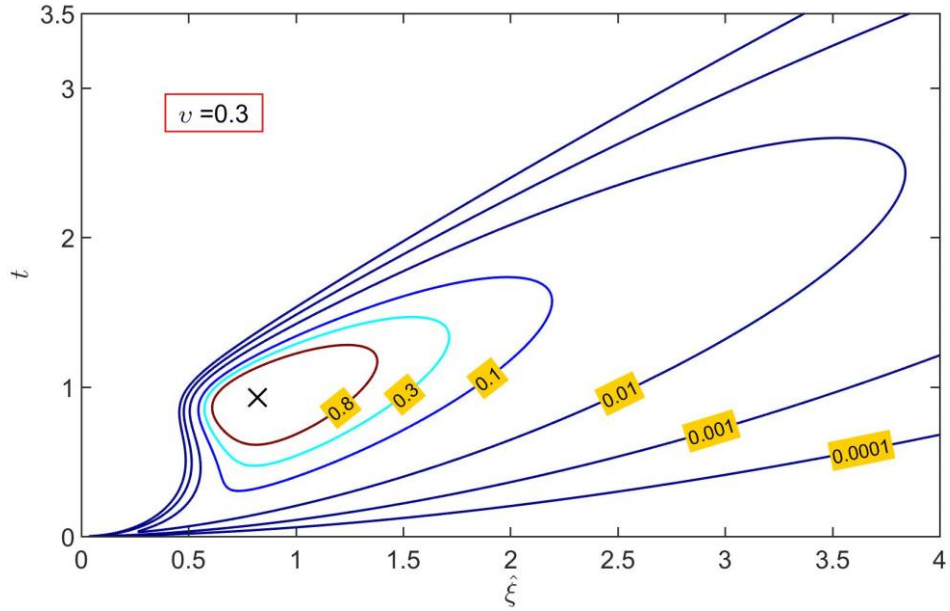

Figure 7(b)

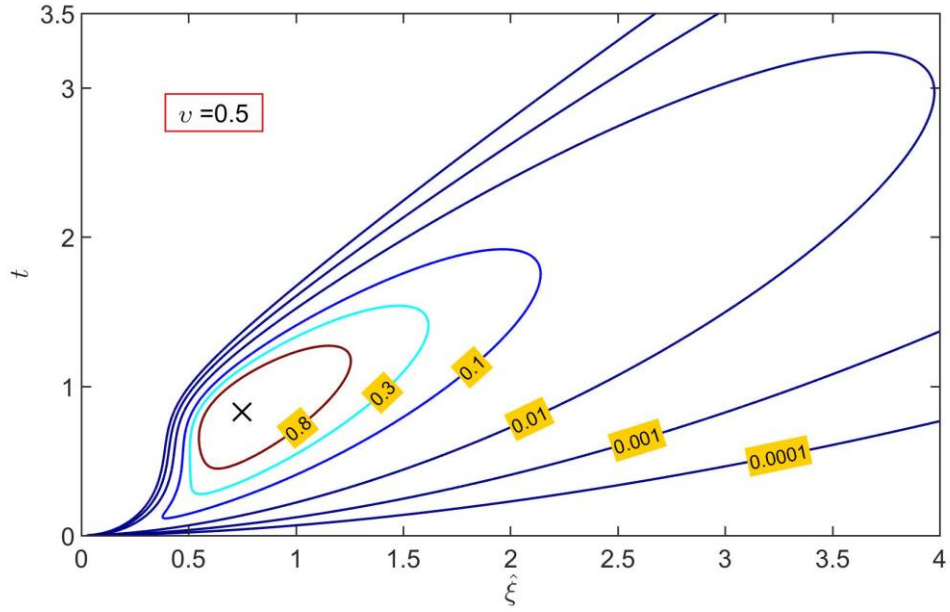

Figure 7(c)

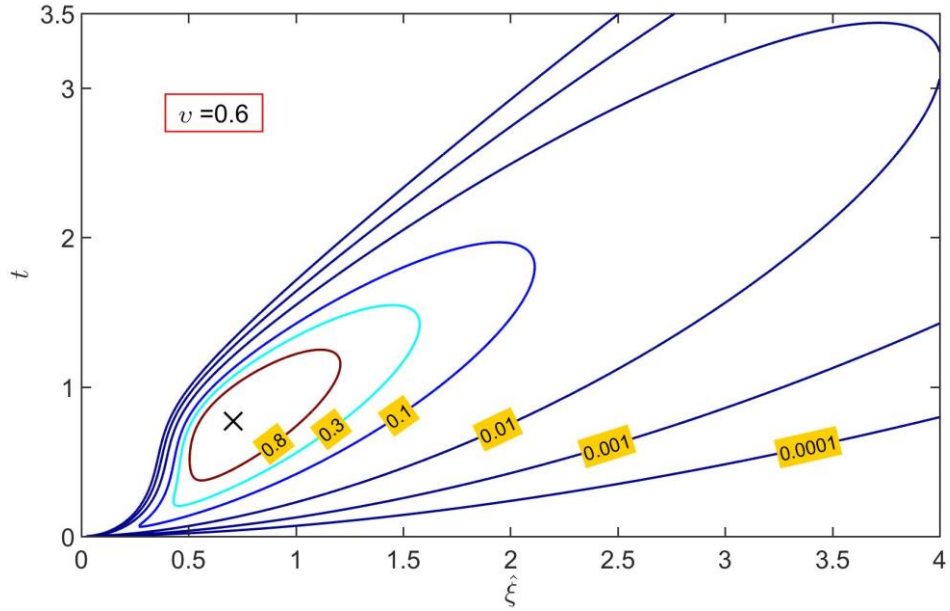

Figure 7(d)

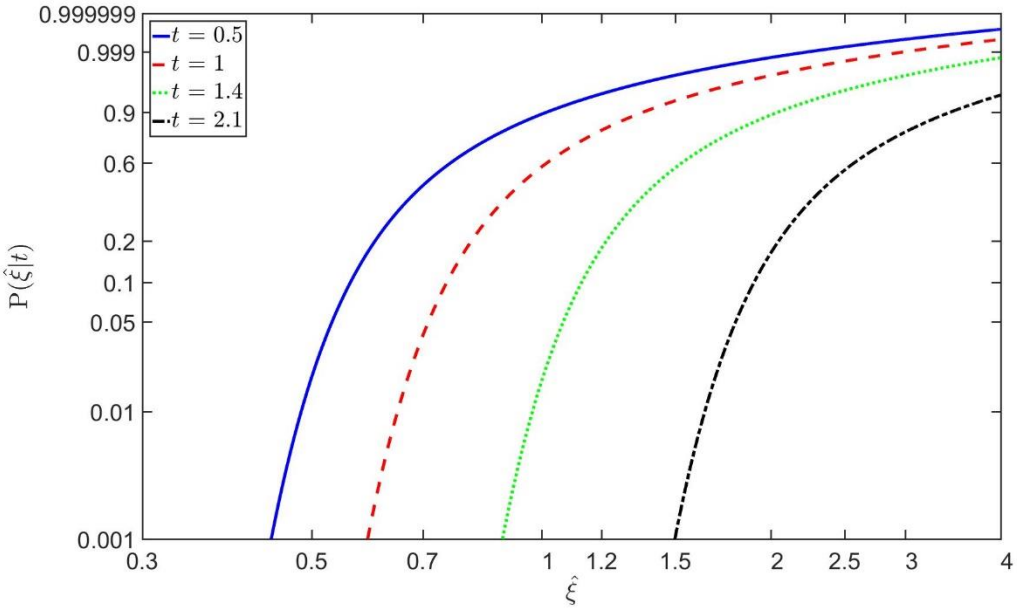

Figure 8

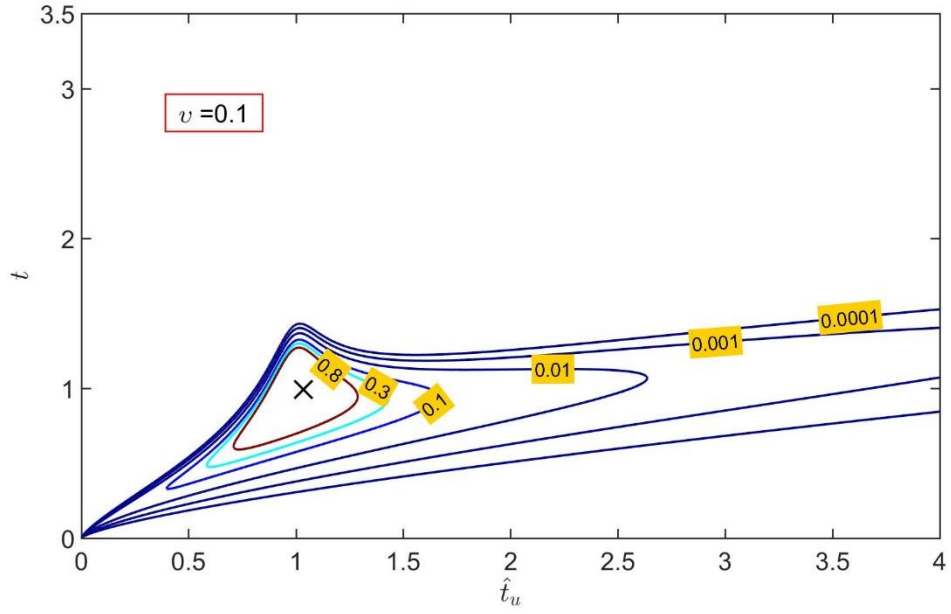

Figure 9(a)

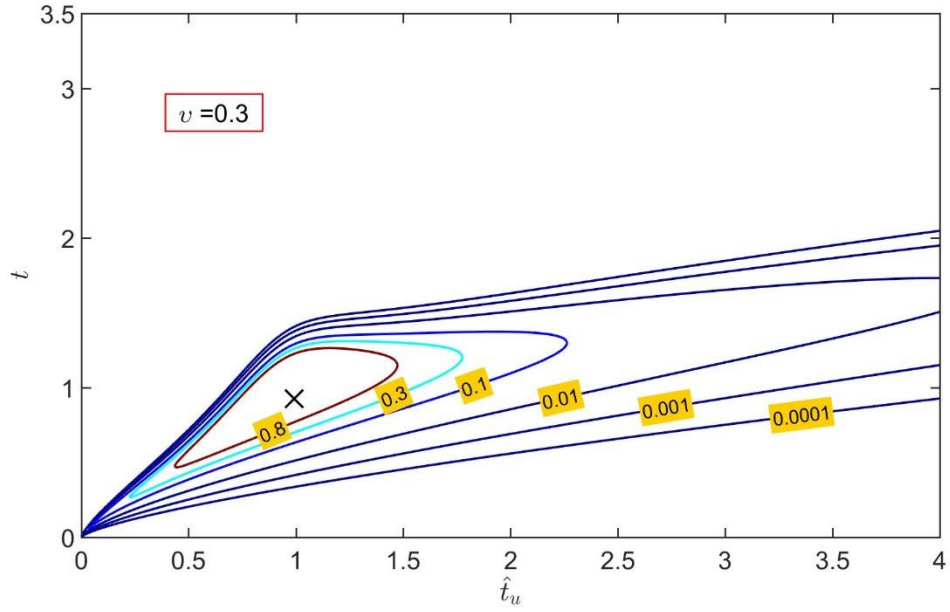

Figure 9(b)

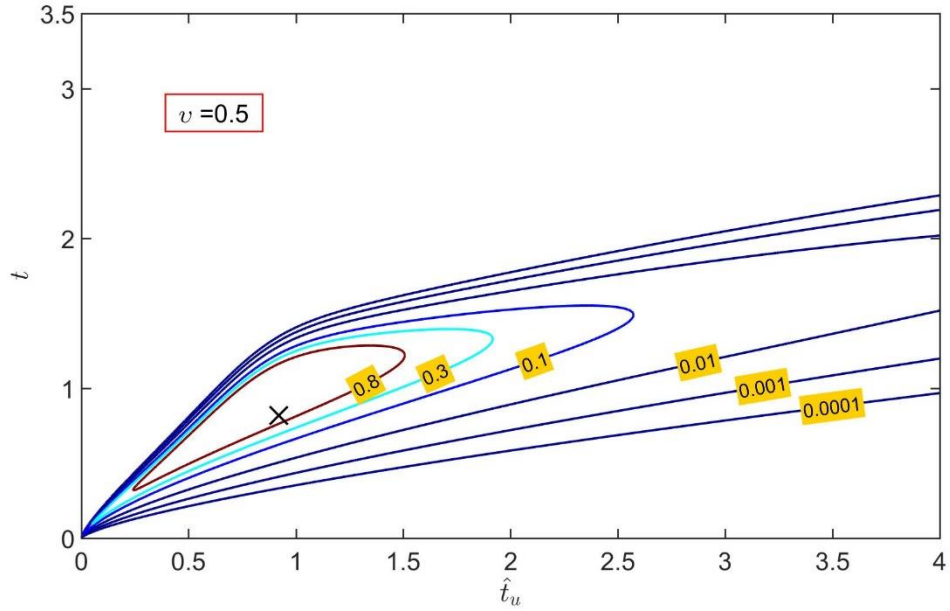

Figure 9(c)

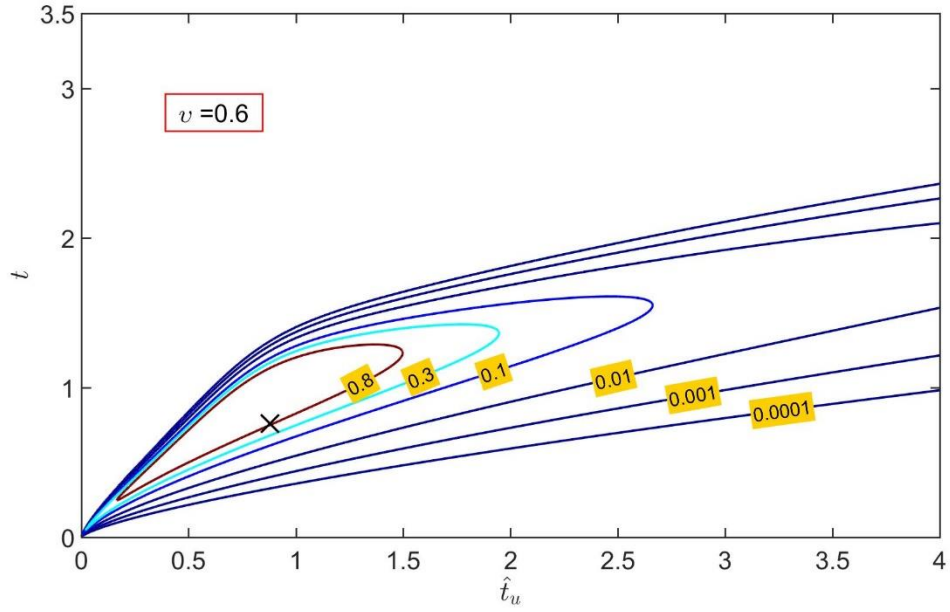

Figure 9(d)

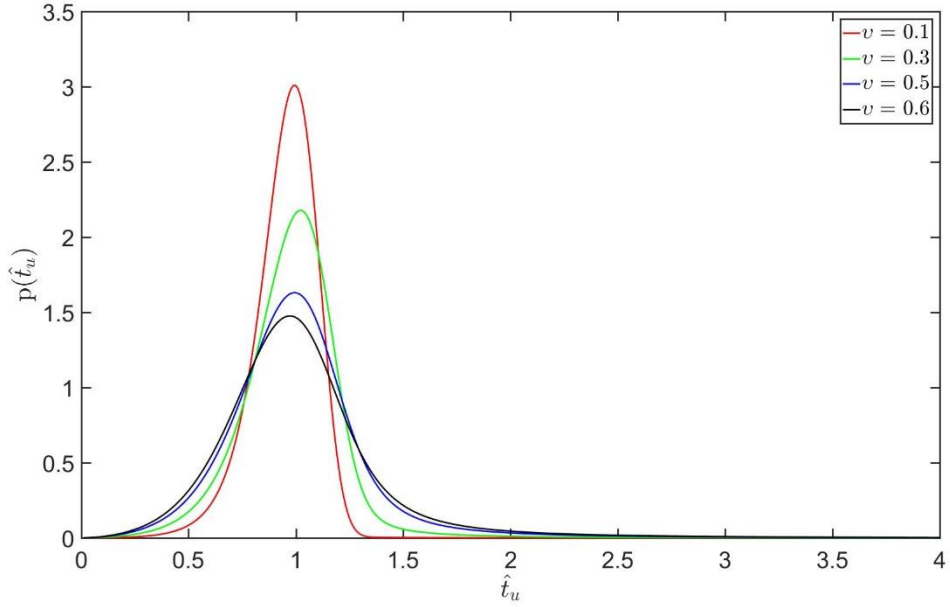

Figure 10

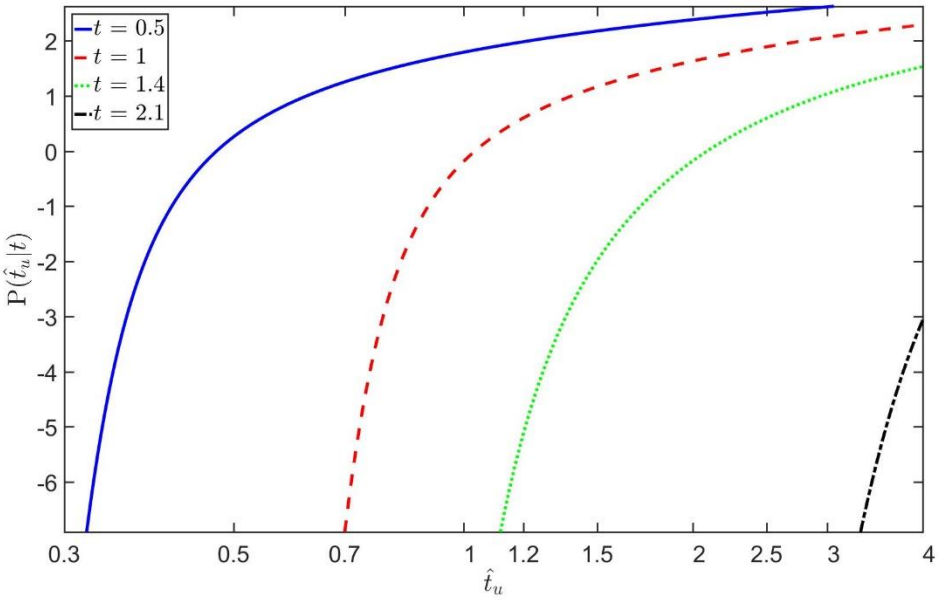

Figure 11

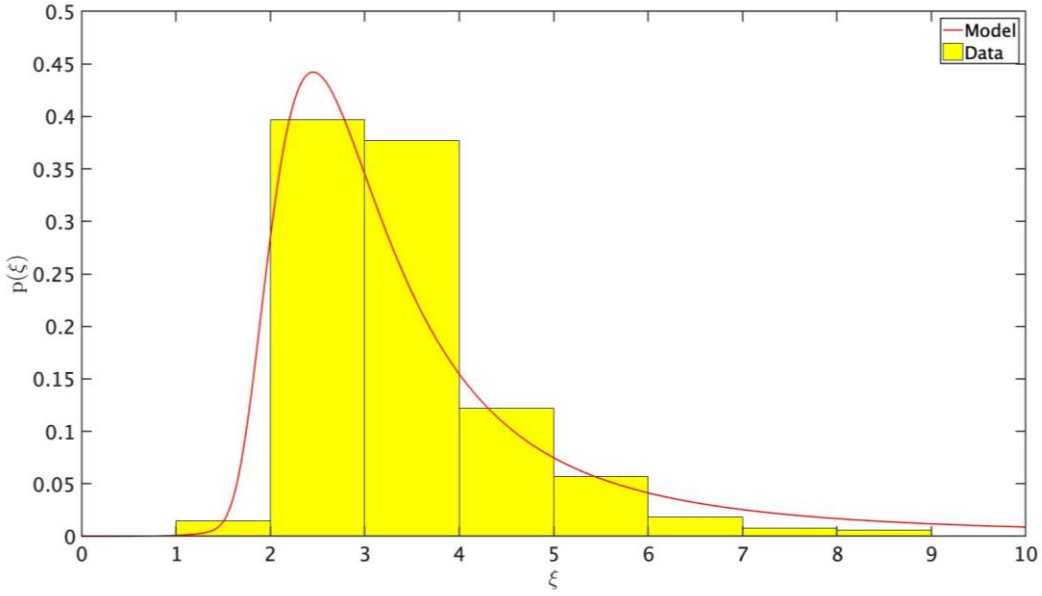

Figure 12